



# Nanotube mode-locked, wavelength and pulsewidth tunable thulium fiber laser

RUIHONG DAI,<sup>1,5</sup> YAFEI MENG,<sup>1,5</sup> YAO LI,<sup>1,4</sup> JIARONG QIN,<sup>1</sup> SHINING ZHU,<sup>2</sup>  
AND FENGQIU WANG<sup>1,3,\*</sup>

<sup>1</sup>*School of Electronic Science and Engineering and Collaborative Innovation Center of Advanced Microstructures, Nanjing University, Nanjing 210093, China*

<sup>2</sup>*National Laboratory of Solid State Microstructures and School of Physics, Nanjing University, Nanjing 210093, China*

<sup>3</sup>*Key Laboratory of Intelligent Optical Sensing and Manipulation, Ministry of Education, Nanjing University, Nanjing 210093, China*

<sup>4</sup>*liyao@nju.edu.cn*

<sup>5</sup>*These authors contributed equally to this work*

*\*fwang@nju.edu.cn*

**Abstract:** Mode-locked oscillators with highly tunable output characteristics are desirable for a range of applications. Here, with a custom-made tunable filter, we demonstrate a carbon nanotube (CNT) mode-locked thulium fiber laser with widely tunable wavelength, spectral bandwidth, and pulse duration. The demonstrated laser's wavelength tuning range reached 300 nm (from 1733 nm to 2033 nm), which is the widest-ever that was reported for rare-earth ion doped fiber oscillators in the near-infrared. At each wavelength, the pulse duration can be regulated by changing the filter's bandwidth. For example, at ~1902 nm, the pulse duration can be adjusted from 0.9 ps to 6.4 ps (the corresponding output spectral bandwidth from 4.3 nm to 0.6 nm). Furthermore, we experimentally and numerically study the spectral evolution of the mode-locked laser in presence of a tunable filter, a topic that has not been thoroughly investigated for thulium-doped fiber lasers. The detailed dynamical change of the mode-locked spectra is presented and we observed gradual suppression of the Kelly sidebands as the filter's bandwidth is reduced. Further, using the polarization-maintaining (PM) cavity ensures that the laser is stable and the output laser's polarization extinction ratio is measured to exceed 20 dB.

© 2019 Optical Society of America under the terms of the [OSA Open Access Publishing Agreement](#)

## 1. Introduction

For a wide range of applications, including optical parametric oscillation (OPO), frequency comb and nonlinear photon spectroscopy [1–5], ultrafast lasers with a fixed wavelength and pulse duration are increasingly unable to meet emerging technical requirements. As a result, tunable ultrafast lasers have received wide attention over the past decades. A number of techniques have been proven to be effective for realizing wavelength and pulsewidth tunable operation, but most are achieved for 1.5  $\mu\text{m}$  cavity [6–10]. For the 2 micron band, where thulium fiber provides a desirably broad emission bandwidth spanning 1.7–2.1  $\mu\text{m}$  and emerging applications for sensing and communications abound, there are still very few reports. Thusfar, most wavelength tunable 2  $\mu\text{m}$  mode locked oscillators are based on birefringence induced filters [11–13]. By the use of a curvature multimode interference filter (MMIF), a mode-locked laser with an output wavelength tuning range of 95 nm was achieved [11]. Moreover, a 60 nm tunable mode-locked  $\text{Tm}^{3+}$  doped fiber laser was demonstrated with a graphene saturable absorber on microfiber [12]. By NPE, a widely tunable mode locked thulium-doped fiber laser with a tuning range from 1842 nm to 1978 nm was reported [13]. However, the fiber birefringence is very sensitive to external perturbations [14], which limits the stability and repeatability of wavelength tuning operation. By contrast, it is simpler and more stable to insert

a tunable bandpass filter (TBF) in the cavity to achieve wavelength tuning [15–17]. By inserting a tunable filter in the cavity, a 120 nm tuning range can be obtained in a Tm-doped fiber laser mode locked with SESAM [16]. With the help of a diffraction grating, a carbon nanotube mode-locked fiber laser tunable from 1860 nm to 2060 nm was reported, corresponding to a 200 nm tuning range [17]. Recently, Woodward et al. have demonstrated a 330 nm tuning range dysprosium doped fiber laser at 3  $\mu\text{m}$  mode-locked by frequency shifted feedback (FSF) [18]. However, all of the works mentioned above demonstrate only wavelength tuning. No work has been reported to achieve a wide pulsewidth tuning in the 2  $\mu\text{m}$  oscillator, except by extra-cavity techniques [19,20].

In addition, with respect to mode-locked Tm-fiber laser, Kelly sidebands are generally considered to be an intrinsic feature of conventional solitons, whose formation is widely attributed to the constructive interference between the soliton pulse and the associated dispersive wave [21,22]. While many aspects of Kelly sidebands are known and can be quantitatively inferred by the total dispersion, cavity length, and pulse duration [23], detailed experimental studies of influence of a bandwidth-tunable filter on mode-locked laser are still rare and incomplete, and such an investigation is best carried out with a broad gain spectrum laser, such as provided by thulium-doped fiber [24].

In this paper, we demonstrate a CNT mode-locked Thulium-doped fiber laser with broadly tunable wavelength and pulse duration. Although there are many novel saturable absorbers (SAs), such as graphene, transition-metal dichalcogenides (TMDs), black phosphorus and etc [25–29], can be used for mode-locking, the CNT thin film SA is chosen in our work because of its easy preparation, stability and broadband nonlinear absorption (due to the distribution of different diameters) [30–32]. The tuning of wavelength and pulse duration is realized through our homemade grating based filter. The maximum tuning range for wavelength is 300 nm (from 1733 nm to 2033 nm). At 1901.8 nm, the pulse duration can be adjusted from 0.9 ps to 6.4 ps (the corresponding spectral bandwidth is from 4.26 nm to 0.64 nm). To the best of our knowledge, it's the first time a 2  $\mu\text{m}$  mode-locked oscillator with both widely tunable wavelength and pulse duration is obtained, and also the tuning range marks the widest ever reported for a mode-locked fiber oscillator in the near-infrared. At the same time, all polarization maintaining structure of the laser ensures strong stability and good self-starting. Moreover, the influence of the filter's bandwidth on mode-locking dynamics was investigated in detail, from both the experimental and numerical perspectives. Our results provide valuable reference for better understanding the interplay of various cavity parameters on mode-locking dynamics.

## 2. Experimental setup

The experimental setup of the laser is shown in Fig. 1. A 1550 nm laser diode (LD) is used as the pump source. The LD has an average output power of 14.2 mW and it can be amplified to 1.5 W by a commercial erbium-doped fiber amplifier (EDFA). Then the 1550 nm pump is coupled into the cavity through a polarization-maintaining 1550/2000 nm fiber wavelength division multiplexer (WDM). A segment of PM TDF (PM-TSF-9/125, Nufern) is used as the gain medium. A dielectric mirror with a reflectivity of 80% is used as one end of the cavity and the 20% transmission is as the output of the laser. Meanwhile, our homemade filter is used as another end mirror with wavelength and spectral bandwidth tunability by changing the horizontal position and slit width respectively. The mode-locking of the Tm-fiber is initiated by the carbon nanotube-carboxymethylcellulose (CNT-CMC) polymer composite film sandwiched between two fiber connectors. A more detailed introduction of the preparation and the properties of the CNT-SA can be referred to our previous work [33].

The total laser cavity length is  $\sim 6.85$  m including 1.87 m active fiber and 4.98 m passive fiber (PM Panda-type fiber). At 2  $\mu\text{m}$ , the dispersion values for the active and passive PM fiber are  $-0.076$  ps<sup>2</sup>/m and  $-0.068$  ps<sup>2</sup>/m respectively. The total cavity dispersion value is  $-0.48$  ps<sup>2</sup>. An optical spectrum analyzer (OSA, Yokogawa AQ6375) and a mid-infrared autocorrelator

(Femtochrome, FR-103XL) is used to measure the output spectrum and pulse duration of the laser. An oscilloscope (Agilent, DSO-X3052A) and a frequency spectrum analyzer (R&S, FSV 30) connected with a high speed photodiode (EOT-5000) are used to measure the output pulse traces and radio frequency spectra. The output power is measured by a power meter (Thorlabs, S148C) and with the help of a PBS, we can also measure the polarization extinction ratio of the output.

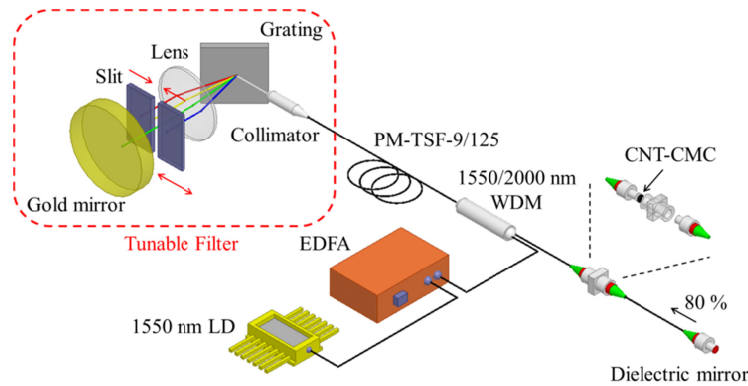


Fig. 1. The schematic setup of the mode-locked fiber laser. LD: laser diode; WDM: wavelength division multiplexer; EDFA: erbium doped fiber amplifier; PM-TSF: polarization maintaining thulium-doped single-mode single clad fiber.

Before characterizing the output of the mode-locked Tm-fiber laser, we tested the performance of the homemade tunable filter with a circulator and an amplified spontaneous emission (ASE) source (NPI Lasers Inc.) at  $2\ \mu\text{m}$ . Figure 2(a) shows the wavelength tuning of the filter. We first fixed the slit width to  $0.2\ \text{mm}$ , corresponding to a filter's bandwidth of  $\sim 4.46\ \text{nm}$ . The center wavelength tuning can be achieved by moving the slit horizontally. Limited by the bandwidth of the ASE laser source used in the test, the measurable center wavelength range is from  $1730\ \text{nm}$  to  $2030\ \text{nm}$  (the filter should have a wider tuning range). Then, in order to characterize the bandwidth tuning of the filter, we fixed the center wavelength at  $1960\ \text{nm}$  and tuned the filter's bandwidth by changing the slit width. Figure 2(b) shows the bandwidth changing continuously from  $2.39\ \text{nm}$  to  $28.13\ \text{nm}$ . From the figure, we can also see that when the bandwidth is narrower than  $\sim 4\ \text{nm}$ , the filter will generate an obvious additional insertion loss. This is mainly due to the relatively large beam diameter from the collimator, so that laser with different wavelengths are mixed together and some part will be blocked by the slit. As a matter of fact, the maximum filter's bandwidth can reach  $220\ \text{nm}$  (see the inset diagram of Fig. 2(b)). Compared to a dielectric mirror with  $100\%$  reflectivity, the insertion loss (by taking account the efficiency of the collimator, grating, lens and gold mirror) of the filter is measured to be around  $3\ \text{dB}$  at  $\sim 2\ \mu\text{m}$ . The measurement is done by using a linearly polarized laser at  $2\ \mu\text{m}$ .

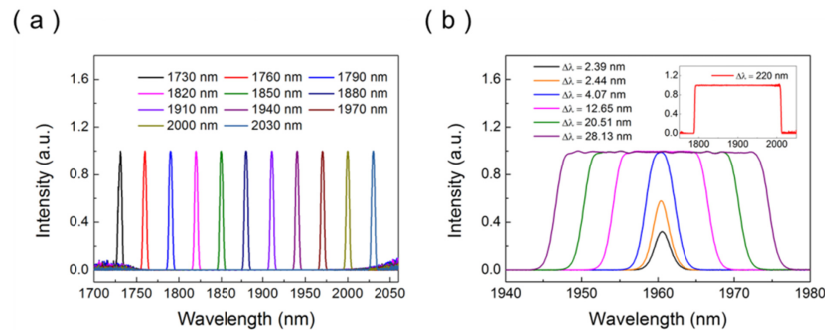


Fig. 2. Tuning characteristics of our tunable filter. (a) The bandwidth is fixed at 4.46 nm, and the wavelength is adjusted from 1730 nm to 2030 nm. (b) The wavelength is fixed at 1960.4 nm, and the bandwidth is adjusted from 2.39 nm to 28.13 nm. Inset: the maximum filter's bandwidth is 220 nm.

### 3. Wavelength and pulsewidth tunable

We first test the laser by fully opening the slit so that no filtering is present in the cavity. Self-started mode-locking of the Tm-doped laser can be obtained by setting the pump power appropriately. Figure 3(a) shows a typical mode-locked pulse train on the oscilloscope. The period of the pulse is 67.5 ns, and the corresponding repetition frequency is 14.83 MHz. To verify the stability of the mode-locking pulse, we measured the radio frequency spectrum of the pulse train. As shown in Fig. 3(b), the signal-to-noise ratio (SNR) is more than 60 dB, confirming a stable mode-locking operation. Since the grating in the cavity is sensitive to the polarization state, there is no need for any other slow axis working devices in the cavity to ensure linear polarization output. By using a PBS, the polarization extinction ratio of the output laser is measured to be more than 20 dB.

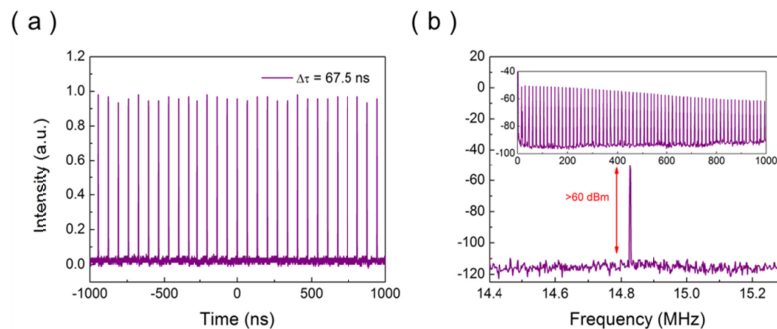


Fig. 3. (a) Output pulse train (corresponding to a repetition rate of 14.83 MHz). (b) Radio frequency spectrum at the fundamental repetition rate ( $f_0 = 14.83$  MHz) with 1 kHz resolution bandwidth. Inset: broadband frequency spectrum (1 GHz span) with 100 kHz resolution bandwidth.

The output spectral properties can be changed by adjusting the position and width of the slit. As shown in Figs. 4(a) and 4(b), we recorded the mode-locked spectra when the wavelength was tuned from 1733 nm to 2033 nm ( $\sim 300$  nm). At each wavelength, the narrowest and widest mode-locking spectrum can be obtained by adjusting the size of the slit. Such a wide wavelength tuning range not only proves that the CNT saturable absorber has a very wide working bandwidth, but also proves that the homemade tunable filter can operate in the entire gain bandwidth of the Thulium-doped fiber with considerable efficiency. The record-level tunability is thus achieved by combining the broadest fiber gain medium together with broadband saturable absorber and tunable filter all in the same laser demonstrator. Figure

4(c) shows the narrowest and widest spectral bandwidth at each wavelength. The bandwidth tuning range is narrower on the two sides of the gain spectrum, which is due to the fact that the gain on both sides is lower. It should be noted that, we need to adjust the pump power to achieve stable mode-locking at different wavelengths. At the edge of the tuning range, greater pump power is required. Figure 4(d) shows the pump power and average output power of the laser for obtaining the narrowest and widest spectral bandwidth. In the mean time, the output power of the oscillator at a fixed wavelength was monitored for 10 hours to characterize its stability. The output power fluctuation of the laser is less than 0.34% which has also proved that the CNT saturable absorber is stable withstand long time illumination.

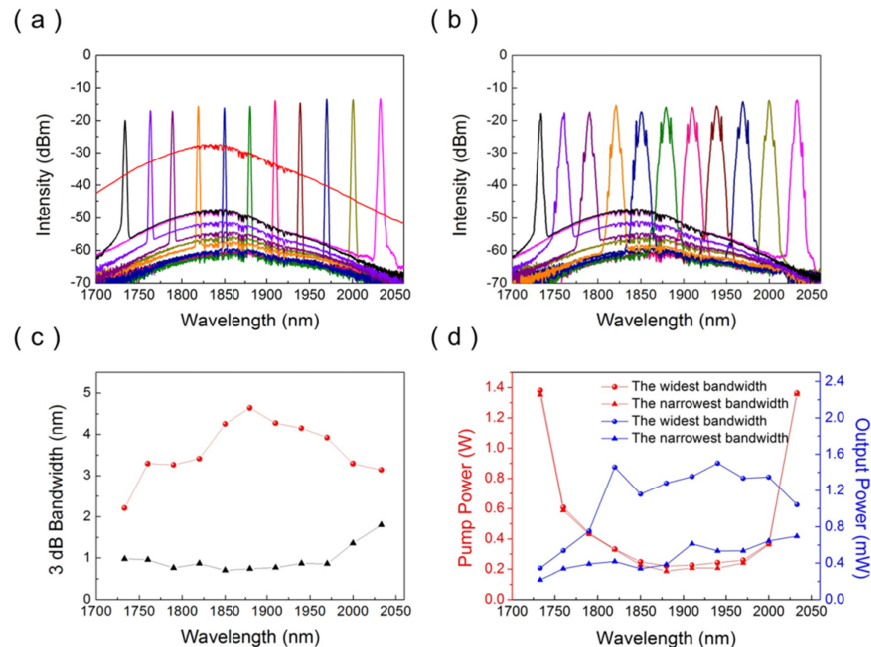


Fig. 4. Wavelength tunability of the mode-locked fiber laser. (a) The narrowest spectral at each wavelength. The red line is the ASE spectrum of the thulium-doped fiber we used. (b) The widest spectral available at each wavelength. (c) The narrowest and widest spectral bandwidth at each wavelength. (d) The pump power and the average output power of the laser at different wavelengths.

Next, we measured the pulse duration at different spectral bandwidth. Figure 5(a) shows the typical autocorrelation trace at  $\sim 1902$  nm, which is about the center of the gain spectrum of the Thulium-doped fiber. Since the average output power of the oscillator is only about 1 mW, not directly measurable from the autocorrelator. We therefore amplified the laser average power to 7 mW by using a thulium doped fiber amplifier (NPI Lasers Inc.). As the output peak power after the amplifier is small (less than 70 W), the variation of the pulse duration in the amplification process can be neglected. As can be seen from Fig. 5(a), the narrowest and widest pulse duration are 0.91 ps and 6.43 ps, and the corresponding spectral bandwidth are 4.26 nm and 0.64 nm respectively. Figure 5(b) illustrated the corresponding spectra with respected to Fig. 5(a). Figure 5(c) shows the experimental pulse duration results corresponding to different spectral bandwidth (the black curve corresponds to the case of hyperbolic secant pulse). It is worth noting that the values of the time bandwidth product (TBP) are very close to 0.315, confirming soliton-like *Sech*<sup>2</sup> pulses. However, in some literatures, it is reported that the value of TBP will increase with the decrease of filter bandwidth, and eventually the value of TBP reaches about 0.45 [10]. But the value of TBP in this paper remains basically the same, which may be caused by different passband shapes of the filter. In addition, similar TBP results

are also obtained when the laser are working at other center wavelengths. Therefore, the pulse duration tuning at each wavelength can be well controlled by manipulating the spectral bandwidth.

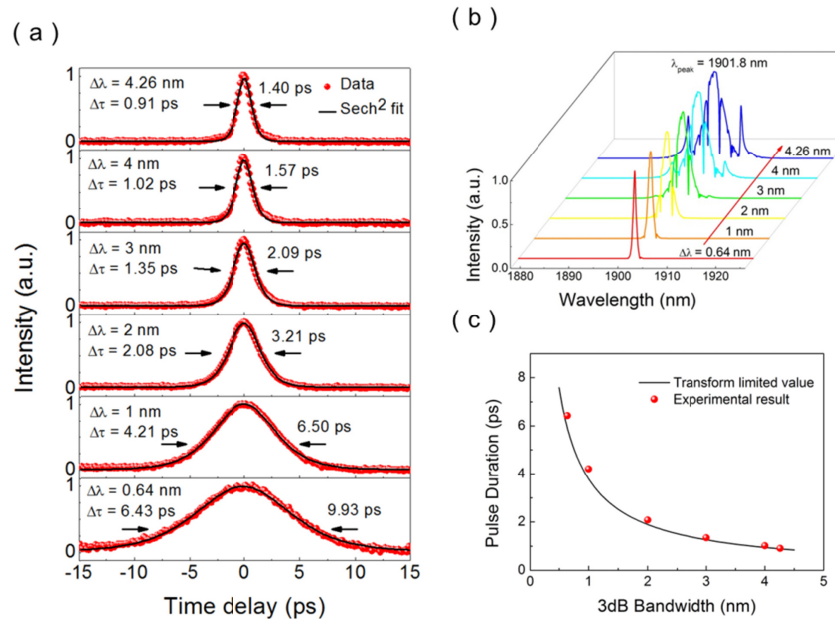


Fig. 5. Pulse duration tunability of the mode-locked fiber laser at 1901.8 nm. (a) Pulse duration can be adjusted from 0.91 ps to 6.43 ps. (b) FWHM bandwidth is tuned from minimum 0.64 nm to maximum 4.26 nm. (c) Output pulse duration as a function of spectral bandwidth.

#### 4. Mode-locking dynamics with tunable filter

Further, we studied the effect of the tunable filter on the mode-locking spectrum in details. First, we remove the slit from the setup, so the filter function does not apply. In this circumstance, when the pump power reaches 225 mW, stable mode-locking with a large number of Kelly sidebands are generated (see “a” in Fig. 6(a)). The central wavelength of the laser is 1892.6 nm, and the 3 dB bandwidth is 4.42 nm. Then we put back the slit and make sure that the center wavelength of the filter is at 1892.6 nm but with a relatively large bandwidth ( $>50$  nm). When pump power reaches 225 mW, the same spectrum will appear as before. Then we gradually reduced the slit width and observed the evolution of the spectrum. As the filter’s bandwidth decreased to about 40 nm, the number of Kelly sidebands began to decrease. But the changes in spectral bandwidth was not obvious (see “b” – “c”). When the filter’s bandwidth is reduced to 12.8 nm (the laser spectrum bandwidth is 4.36 nm), only two Kelly sidebands are left. (see “c”). By further reducing the filter’s bandwidth, it can be found that the spectral bandwidth of the laser also changes, and the two Kelly sidebands are slowly decreasing until finally disappear (see “c” - “f”). When the filter’s bandwidth is reduced to 2.85 nm, the spectral bandwidth of the laser is only 0.84 nm (see “g”). During the process, the pump power remains unchanged, the only changed parameter is the filter’s bandwidth. The spectrum evolution in the process proves that the filter suppresses the dispersive waves in the cavity, so the original Kelly sidebands will gradually disappear when the filter’s bandwidth is reduced. Figure 6(b) shows the spectral width, pulse duration and output power as a function of the filter’s bandwidth. It is noted when the filter’s bandwidth is reduced from 40 nm to 12.8 nm, the Kelly sidebands have little effect on the pulse duration as the output spectral width hardly changes. There are some works that have been studied about the generation of the sidebands. It is

believed that the soliton sidebands are observed when the cavity length exceeds the soliton period, which means that disturbances are not averaged out and dispersive waves are shed by the soliton [34–36]. With respect to our work, when the filter bandwidth began to decrease, there was no significant change in the pulsewidth in the beginning (the soliton period is almost constant), while the number of sidebands decreased significantly. We think that it may be just the presence of a filter that removes the dispersive wave in the cavity. Similar result has also been reported in [37], while the Kelly sidebands are suppressed by just changing the polarization states.

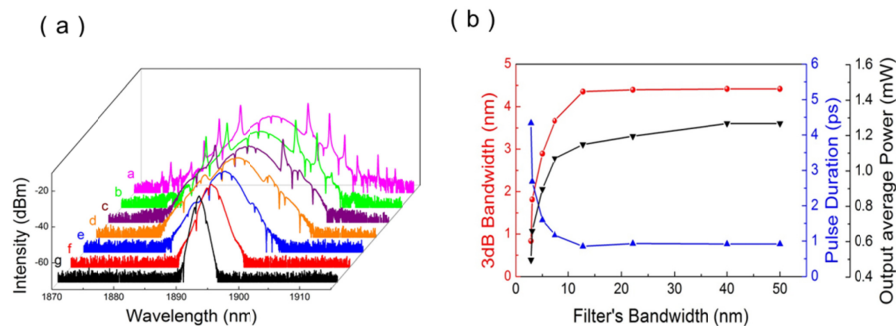


Fig. 6. (a) The evolution of the spectrum when the filter's bandwidth is decreased. (b) Output spectrum bandwidth, pulse duration and average power as a function of the filter's bandwidth.

In order to retrieve the effect of the filter on output performance of the mode-locked Tm-fiber laser, we carried out a numerical simulation to verify the experimental results. The numerical simulation was done with a commercial software by solving the extended nonlinear Schrödinger equation by the split-step Fourier method [38]. Linear effects including saturable gain, loss and dispersion, and nonlinear effects including SPM, Raman, self steepening were taken into account. The reflectivity of the SA is given by  $R = R_0 + \Delta R / (1 + |A(T)|^2 / P_A)$  where  $R_0$  (linear reflectivity) is 65%,  $\Delta R$  (saturable reflection coefficient) is 35%,  $P_A$  (absorber saturation power coefficient) is 100 W.

Single-pulse soliton propagation is seen to start from quantum noise and was executed in loop until a steady state was reached. Figure 7 shows the simulated output spectra and autocorrelation traces under different filter's bandwidth. The simulation results are in good agreement with the experimental results. When the filter is not included, multiple Kelly bands are clearly discernable in the frequency domain (as "a" in Fig. 7(a)), since the total dispersion of the fiber in the cavity is negative. When the filter is included and the bandwidth is reduced, the number of Kelly sidebands is reduced first, while the 3 dB bandwidth of the spectrum is almost unchanged. Simultaneously, the corresponding pulse width doesn't change much either. Afterwards, when the filter's bandwidth is further reduced, the Kelly sidebands gradually disappeared. The 3 dB bandwidth of the output spectrum also decreased and the pulse width gradually increased. Moreover, during the entire process, the values of TBP are all approximately around 0.315, similar to the experimental results.

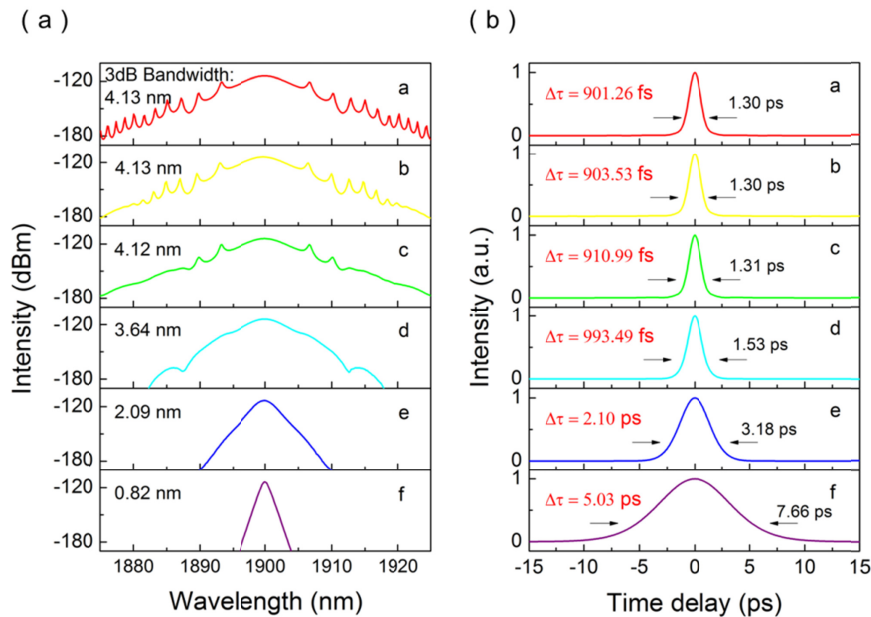


Fig. 7. Simulation results. (a) Spectra at different filter's bandwidth. a: without filter; b: 35.2 nm filter; c: 20.5 nm; d: 8.0 nm; e: 4.1 nm; f: 2.9 nm. (b) The corresponding simulated autocorrelation traces.

## 5. Conclusion

We report an ultrashort thulium doped fiber laser with both wavelength and pulse duration tunable in a wide range. The center wavelength can be adjusted from 1733 nm to 2033 nm (300 nm). As far as we know, this is the widest wavelength tuning results ever achieved for mode-locked fiber oscillators in the near-infrared. For a specified wavelength, the pulse duration can be tuned within a desirable range, *i.e.* from 0.91 ps to 6.43 ps, by controlling the filter's bandwidth. We have also experimentally and numerically studied the pulse dynamics of the mode-locked laser with tunable filter and investigated the effect of the filter on the Kelly sidebands, providing additional insights into the interplay between soliton and dispersive waves. Moreover, as all the devices used in the cavity are polarization-maintaining, the fiber laser exhibits good mode-locking stability and repeatability. Such a fiber laser with wide tunability at 2  $\mu\text{m}$  are valuable in various applications, such as spectroscopy, medical sensing and diagnostics, as well as optical fiber or free-space communications.

## Funding

National Key R&D Program of China (2017YFA0206304); the National Basic Research Program of China (2014CB921101); National Natural Science Foundation of China (61775093, 61378025, 61427812, 61805116); a Jiangsu Shuangchuang Team Program; Natural Science Foundation of Jiangsu Province (BK20170012, BK20140612, BK20180056).

## References

1. N. Leindecker, A. Marandi, R. L. Byer, K. L. Vodopyanov, J. Jiang, I. Hartl, M. Fermann, and P. G. Schunemann, "Octave-spanning ultrafast OPO with 26-61  $\mu\text{m}$  instantaneous bandwidth pumped by femtosecond Tm-fiber laser," *Opt. Express* **20**(7), 7046 (2012).
2. D. Sánchez, M. Hemmer, M. Baudisch, K. Zawilski, P. Schunemann, H. Hoogland, R. Holzwarth, and J. Biegert, "Broadband mid-IR frequency comb with CdSiP<sub>2</sub> and AgGaS<sub>2</sub> from an Er,Tm:Ho fiber laser," *Opt. Lett.* **39**(24), 6883–6886 (2014).
3. A. Schliesser, N. Picqué, and T. W. Hänsch, "Mid-infrared frequency combs," *Nat. Photonics* **6**(7), 440–449 (2012).

4. S. A. Studenikin and M. Cocivera, "Time-resolved luminescence and photoconductivity of polycrystalline ZnO films," *J. Appl. Phys.* **91**(8), 5060–5065 (2002).
5. Z. Cheng, C. Qin, F. Wang, H. He, and K. Goda, "Progress on mid-IR graphene photonics and biochemical applications," *Front Optoelectron.* **9**(2), 259–269 (2016).
6. F. Wang, A. G. Rozhin, V. Scardaci, Z. Sun, F. Hennrich, I. H. White, W. I. Milne, and A. C. Ferrari, "Wideband-tunable, nanotube mode-locked, fibre laser," *Nat. Nanotechnol.* **3**(12), 738–742 (2008).
7. Y. Liu, X. Zhao, J. Liu, G. Hu, Z. Gong, and Z. Zheng, "Widely-pulsewidth-tunable ultrashort pulse generation from a birefringent carbon nanotube mode-locked fiber laser," *Opt. Express* **22**(17), 21012–21017 (2014).
8. Z. Yan, H. Wang, K. Zhou, Y. Wang, C. Li, W. Zhao, and L. Zhang, "Soliton mode locking fiber laser with an all-fiber polarization interference filter," *Opt. Lett.* **37**(21), 4522–4524 (2012).
9. H. Zhang, D. Y. Tang, R. J. Knize, L. M. Zhao, Q. L. Bao, and K. P. Loh, "Graphene mode locked, wavelength-tunable, dissipative soliton fiber laser," *Appl. Phys. Lett.* **96**(11), 111112 (2010).
10. D. Li, H. Jussila, Y. Wang, G. Hu, T. Albrow-Owen, R. C. T. Howe, Z. Ren, J. Bai, T. Hasan, and Z. Sun, "Wavelength and pulse duration tunable ultrafast fiber laser mode-locked with carbon nanotubes," *Sci. Rep.* **8**(1), 2738 (2018).
11. N. Li, M. Y. Liu, X. J. Gao, L. Zhang, Z. X. Jia, Y. Feng, Y. Ohishi, G. S. Qin, and W. P. Qin, "All-fiber widely tunable mode-locked thulium-doped laser using a curvature multimode interference filter," *Laser Phys. Lett.* **13**(7), 075103 (2016).
12. G. Yang, Y. G. Liu, Z. Wang, J. C. Lou, Z. H. Wang, and Z. B. Liu, "Broadband wavelength tunable modelocked thulium-doped fiber laser operating in the 2  $\mu$ m region by using a graphene saturable absorber on microfiber," *Laser Phys. Lett.* **13**(6), 065105 (2016).
13. Z. Yan, X. Li, Y. Tang, P. P. Shum, X. Yu, Y. Zhang, and Q. J. Wang, "Tunable and switchable dual-wavelength Tm-doped mode-locked fiber laser by nonlinear polarization evolution," *Opt. Express* **23**(4), 4369–4376 (2015).
14. G. P. Agrawal, "*Applications of Nonlinear Fiber Optics*," Fourth ed., (Academic Press, Boston, 2007).
15. F. Wang, Y. Meng, E. Kelleher, G. Guo, Y. Li, Y. Xu, and S. Zhu, "Stable gain-switched thulium fiber laser with 140 nm tuning range," *IEEE Photonics Technol. Lett.* **28**(12), 1340–1343 (2016).
16. Z. Xu, Z. Y. Dou, J. Hou, and X. J. Xu, "All-fiber wavelength-tunable Tm-doped fiber laser mode locked by SESAM with 120 nm tuning range," *Appl. Opt.* **56**(21), 5978–5981 (2017).
17. Y. Meng, Y. Li, Y. Xu, and F. Wang, "Carbon nanotube mode-locked thulium fiber laser with 200 nm tuning range," *Sci. Rep.* **7**(1), 45109 (2017).
18. R. I. Woodward, M. R. Majewski, and S. D. Jackson, "Mode-locked dysprosium fiber laser: Picosecond pulse generation from 2.97 to 3.30  $\mu$ m," *APL Photonics* **3**(11), 116106 (2018).
19. Y. T. Lin and G. R. Lin, "Dual-stage soliton compression of a self-started additive pulse mode-locked erbium-doped fiber laser for 48 fs pulse generation," *Opt. Lett.* **31**(10), 1382–1384 (2006).
20. M. Wang, H. Zhang, R. Wei, Z. Zhu, S. Ruan, P. Yan, J. Wang, T. Hasan, and Z. Sun, "172 fs, 24.3 kW peak power pulse generation from a Ho-doped fiber laser system," *Opt. Lett.* **43**(19), 4619–4622 (2018).
21. S. M. J. Kelly, "Characteristic sideband instability of periodically amplified average soliton," *Electron. Lett.* **28**(8), 806–807 (1992).
22. W. C. Chen, W. C. Xu, F. Song, M. C. Shen, D. A. Han, and L. B. Chen, "Vector solitons in femtosecond fibre lasers," *Eur. Phys. J. D* **48**(2), 255–260 (2008).
23. M. L. Dennis and I. N. Duling III, "Experimental study of sideband generation in femtosecond fiber laser," *IEEE J. Quantum Electron.* **30**(6), 1469–1477 (1994).
24. S. D. Jackson, "Towards high-power mid-infrared emission from a fiber laser," *Nat. Photonics* **6**(7), 423–431 (2012).
25. F. Wang, F. Torrisi, Z. Jiang, D. Popa, T. Hasan, Z. Sun, W. Cho, and A. C. Ferrari, "Graphene passively Q-switched two-micron fiber lasers," in *Conference on Lasers and Electro-Optics 2012 (Optical Society of America, San Jose, California, 2012)*, P. JW2A.72.
26. L. Lu, Z. Liang, L. Wu, Y. Chen, Y. Song, S. C. Dhanabalan, J. S. Ponraj, B. Dong, Y. Xiang, F. Xing, D. Fan, and H. Zhang, "Few-layer bismuthene: Sonochemical exfoliation, nonlinear optics and applications for ultrafast photonics with enhanced stability," *Laser Photonics Rev.* **12**(1), 1700221 (2018).
27. Z. Wang, Y. Chen, C. Zhao, H. Zhang, and S. Wen, "Switchable dual-wavelength synchronously Q-switched Erbium-doped fiber laser based on graphene saturable absorber," *IEEE Photonics J.* **4**(3), 869–876 (2012).
28. J. Ma, S. Lu, Z. Guo, X. Xu, H. Zhang, D. Tang, and D. Fan, "Few-layer black phosphorus based saturable absorber mirror for pulsed solid-state lasers," *Opt. Express* **23**(17), 22643–22648 (2015).
29. X. Jiang, S. Liu, W. Liang, S. Luo, Z. He, Y. Ge, H. Wang, R. Cao, F. Zhang, Q. Wen, J. Li, Q. Bao, D. Fan, and H. Zhang, "Broadband nonlinear photonics in few-layer MXene  $Ti_3C_2T_x$  (T = F, O, or OH) nanosheets," *Laser Photonics Rev.* **12**(2), 1700229 (2018).
30. F. Wang, A. G. Rozhin, Z. Sun, V. Scardaci, I. H. White, and A. C. Ferrari, "Soliton fiber laser mode-locked by a single-wall carbon nanotube-polymer composite," *Phys. Status Solidi, B Basic Res.* **245**(10), 2319–2322 (2008).
31. V. Scardaci, A. G. Rozhin, P. H. Tan, F. Wang, I. H. White, W. I. Milne, and A. C. Ferrari, "Carbon nanotubes for ultrafast photonics," *Phys. Status Solidi, B Basic Res.* **244**(11), 4303–4307 (2007).
32. W. Li, T. Du, J. Lan, C. Guo, Y. Cheng, H. Xu, C. Zhu, F. Wang, Z. Luo, and Z. Cai, "716 nm deep-red passively Q-switched Pr:ZBLAN all-fiber laser using a carbon-nanotube saturable absorber," *Opt. Lett.* **42**(4), 671–674 (2017).

33. S. Xu, F. Wang, C. Zhu, Y. Meng, Y. Liu, W. Liu, J. Tang, K. Liu, G. Hu, R. C. Howe, T. Hasan, R. Zhang, Y. Shi, and Y. Xu, "Ultrafast nonlinear photoresponse of single-wall carbon nanotubes: a broadband degenerate investigation," *Nanoscale* **8**(17), 9304–9309 (2016).
34. S. M. J. Kelly, K. Smith, K. J. Blow, and N. J. Doran, "Average soliton dynamics of a high-gain erbium fiber laser," *Opt. Lett.* **16**(17), 1337–1339 (1991).
35. N. Pandit, D. U. Noske, S. M. J. Kelly, and J. R. Taylor, "Characteristic instability of fiber loop soliton lasers," *Electron. Lett.* **28**(5), 455–457 (1992).
36. D. U. Noske and J. R. Taylor, "Spectral and temporal stabilization of a diode-pumped ytterbium-erbium fiber soliton laser," *Electron. Lett.* **29**(25), 2200–2201 (1993).
37. Z. Luo, A. Luo, W. Xu, C. Song, Y. Gao, and W. Chen, "Sideband controllable soliton all-fiber ring laser passively mode-locked by nonlinear polarization rotation," *Laser Phys. Lett.* **6**(8), 582–585 (2009).
38. <http://www.fiberdesk.com/>.